JOURNAL OF THE AMERICAN CHEMICAL SOCIETY

Communication

The Template Synthesis of Double Coaxial Carbon Nanotubes with Nitrogen-Doped and Boron-Doped Multiwalls

Yang, Xu, Akira Tomita, and Takashi Kyotani

J. Am. Chem. Soc., **2005**, 127 (25), 8956-8957• DOI: 10.1021/ja052357e • Publication Date (Web): 01 June 2005

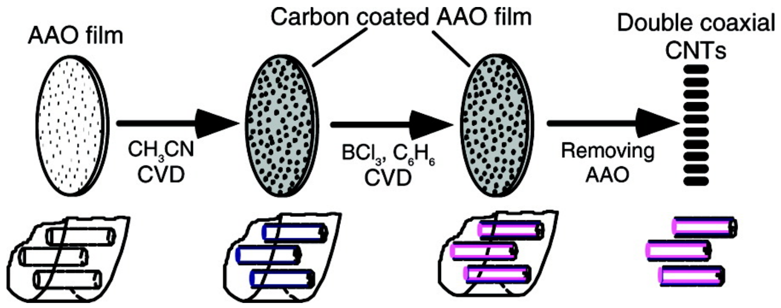

Journal of the American Chemical Society is published by the American Chemical Society. 1155 Sixteenth Street N.W., Washington, DC 20036

J|A|C|S
COMMUNICATIONS

The Template Synthesis of Double Coaxial Carbon Nanotubes with Nitrogen-Doped and Boron-Doped Multiwalls

Quanhong Yang, Weihua Xu, Akira Tomita, and Takashi Kyotani*

Institute of Multidisciplinary Research for Advanced Materials, Tohoku University, Sendai 980-8577, Japan

Received April 12, 2005; E-mail: kyotani@tagen.tohoku.ac.jp

With the miniaturization of silicon-based semiconducting devices now appearing at its limits, development of other kinds of devices of smaller size (nanodevices) becomes urgent for the next generation of electronics. Low-dimensional carbon materials, especially carbon nanotubes (CNTs), are believed to be one of the most potential alternatives to silicon. Constituting carbon-based nanoscale diodes or transistors, thus, becomes one of the main topics in CNT-based nanoelectronics.[1] Doping of some kinds of heteroatoms into CNTs may lead to the formation of electron-excess *n*-type (e.g., N-doped CNTs) or electron-deficient *p*-type (e.g., B-doped CNTs) semiconducting nanotubes.[1−3] Provided that one can control, at nanometer level, the position and distribution of such heteroatoms as N and B in CNTs, various types of nanostructured junctions with controlled electronic properties would be possibly prepared. Our group first reported the successful preparation of the double coaxial CNTs of N-doped and undoped multiwalls by the template technique[4] and found dual physicochemical properties in the coaxial structure.[5] Here, we report first synthesis of more interesting materials: double coaxial CNTs composed of N-doped and B-doped multiwalls (hereafter abbreviated as NB-CNTs) using the template technique.

The figure presented in the Table of Contents gives a schematic illustration of the two-step template synthesis of NB-CNTs. Over an array of parallel and straight nanochannels (inner diameter: 30 nm) in an anodic aluminum oxide (AAO) film, acetonitrile CVD (CH_3CN: 21.0 cm^3/min, N_2: 500 cm^3/min) was first conducted at 800 °C for 2 h, leading to the uniform coating of a N-doped carbon layer on the inner walls of the AAO nanochannels. After a heat-treatment in N_2 gas flow (300 cm^3/min) at 950 °C for 1 h, a second-step CVD was carried out on the N-doped carbon-coated AAO film using benzene as the carbon source and boron trichloride as the boron source (C_6H_6: 4.8 cm^3/min, BCl_3: 4.8 cm^3/min, N_2: 150 cm^3/min) at 725 °C for 20 min. This second CVD step gave rise to B-containing carbon deposition on the already-deposited N-doped carbon layer. Then, the heat-treatment was again conducted for the coated AAO under the same conditions as before. By removing the AAO template with HF treatment, the double coaxial NB-CNTs were liberated. Here, several kinds of CNTs (C-CNTs, N-CNTs, and CB-CNTs) were prepared by the template technique for references. C-CNTs and N-CNTs were prepared by propylene CVD and acetonitrile CVD (conditions being the same as the first CVD step of NB-CNTs) at 800 °C and possess undoped and N-doped carbon walls, respectively. CB-CNTs, which have coaxial outer undoped and inner B-doped multiwalls, were prepared by the first propylene CVD (the same as C-CNTs) and the second benzene and boron trichloride CVD (the same as the second CVD of NB-CNTs). Heat-treatment was conducted for all of the samples in N_2 at 950 °C, and HF was used to remove these templates. It should be noted that single-stack B-doped CNTs cannot be prepared by the present technique, possibly due to a direct reaction between BCl_3 and AAO.

The two-step synthesis resulted in bundled CNTs with a uniform length of 70 μm, exactly the same as the thickness of the AAO film used as a template. Figure 1 shows transmission electron microscopy (TEM) images of a single-stack N-CNT and a double-stack coaxial NB-CNT. It is apparent that both the CVD processes resulted in the uniform deposition of the carbon layers (N-CNT: 1.5 nm, NB-CNT: 5.0 nm). In other words, NB-CNTs have coaxial carbon layers, the outer (1.5 nm of thickness, about 4 carbon layers) and the inner (3.5 nm, about 10 carbon layers) layers being prepared by the first and second step of CVD, respectively. The high-resolution TEM (HRTEM) image (the inset of Figure 1b) reveals that the coaxial CNT contains discontinued and roughly parallel graphene planes, and there is no visible difference between the outer and inner layers prepared by the different CVD steps (4 N-doped and 10 B-doped layers are roughly distinguished from each other by the dotted line).

X-ray photoelectron spectroscopy (XPS) was used to characterize the surface composition of inner and outer layers of NB-CNTs. Generally, an XPS spectrum mainly reflects the information of the outer layer of the measured specimen, and it is difficult to reflect the information from its inner layer. However, in the case of the double coaxial nanotubes, NB-CNTs, the characteristics of their inner surface (inner layer) can be estimated from the analyses of the external surface (upper layer) of the corresponding carbon-coated AAO (abbreviated as NB/AAO), as pointed out in the previous communication.[4] We thus regard an XPS spectrum of the coated AAO film as that of the inner surface (inner layer) of the resulting nanotubes. As shown in Figure 2, the XPS spectra of NB/AAO (inner layer of resulting NB-CNTs) are characterized by a large B_{1s} peak without any N_{1s} peaks, while the resulting nanotubes, NB-CNTs, possess a sound N_{1s} peak with a very small B_{1s} peak. It is thus easy to conclude that NB-CNTs have coaxial sidewall structure of outer N-doped (N/C atomic ratio: 0.025) and inner B-doped layers (B/C: 0.040). Further analyses of the N_{1s} and B_{1s} spectra reveal that N atoms in the outer layer mainly exist as quaternary N with a small portion in pyridinic N, while most of the B atoms in the inner layer are bound to C to form B−C bonds. These findings indicate that both N and B substitute some carbon atoms in graphene planes in sidewalls of CNTs.

We compared crystallinity of NB-CNTs with that of the three reference samples, C-CNTs, N-CNTs, and CB-CNTs, based on XRD analyses (as shown in Table 1), and found that, among the four samples, C-CNTs have the highest (the lowest interlayer spacing and the largest crystal size) and N-CNTs have the lowest crystallinity. Two points should be noted. On one hand, N- or B-doping into the carbon layer decreases the crystallinity of the carbon layer since all kinds of doped CNTs are less crystallized than C-CNTs. On the other hand, the crystallinity of N-CNTs is a little lower than that of NB-CNTs. These findings suggest that both the coaxial layers in NB-CNTs are less crystallized than the undoped

10.1021/ja052357e CCC: $30.25

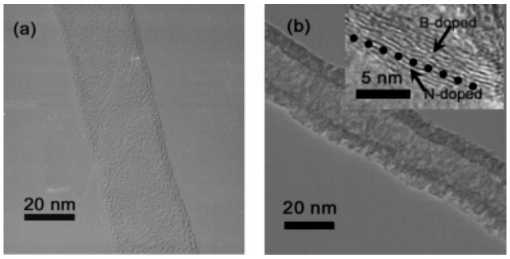

Figure 1. TEM images of (a) an N-CNT and (b) an NB-CNT. Inset of (b): HRTEM image of the wall of an NB-CNT.

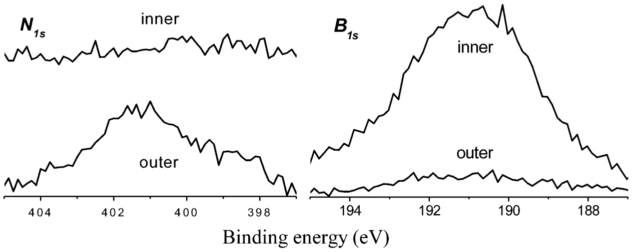

Figure 2. N_{1s} and B_{1s} XPS spectra of NB/AAO (inner layer of NB-CNT) and NB-CNT (outer layer).

Table 1. Structural Parameters and Physicochemical Properties of Template-Synthesized Carbon Nanotubes

	C-CNTs	N-CNTs	CB-CNTs	NB-CNTs
d_{002} (nm)[a]	0.341	0.359	0.350	0.355
L_c (nm)[b]	4.0	1.6	3.0	2.1
O_2 adsorption capacity (μmol/g)	70	350	90	120
electrical resistivity (Ω·cm)	1.8×10^3	1.6×10	1.5×10	5.5

[a] Interlayer distance between graphene planes. [b] The crystalline sizes were determined from the (002) peaks of the XRD patterns of the CNTs.

carbon layers, and the N-doped outer layer is slightly less crystallized than the B-doped inner layer.

O_2 chemisorption measurement was also conducted on NB-CNTs and the reference samples. All of the samples were heat-treated under a He flow at 950 °C for 1 h to clean the sample surface and were then subjected to an O_2 chemisorption at 200 °C, followed by a temperature-programmed desorption (TPD) measurement, where CO_2 and CO gases liberated from the CNTs were quantitatively monitored by a high-speed gas chromatograph. Accordingly, O_2 chemisorption capacities of all of the samples were determined. Based in Table 1, N-CNTs have a chemisorption capacity about 5 times greater than that of C-CNTs and 3 times greater than that of NB-CNTs, while CB-CNTs have activity comparable to that of C-CNTs. It means that the N-doping makes a great contribution, but B-doping has little contribution to the increase in chemical activity. Also, it is concluded that, despite a small crystallinity difference between the two layers, NB-CNTs have entirely different chemical properties at the inner and outer layers of the tubular structure.

Doping N or B into carbon layers is believed to modify the electronic structure and, thereby, electrical conductivity properties. We measured the electrical resistance of NB-CNTs using a simple two-terminal method, as presented in ref 5. The nanotubes prepared by our template technique are embedded in the nanochannels of AAO templates, being parallel to each other and vertical to the outer surface of the templates. We coated both sides of a CNT−AAO composite film with a silver paste, to which two silver wires were attached. A potential (−1.0 to 1.0 V) is applied to both surfaces of the film through the two conducting wires, and its $I-V$ characteristics were measured at 25 °C. The $I-V$ characteristics of the carbon-coated AAO films are of ohmic nature, and hence, the resistances of the coated AAO were obtained from the slopes of the $I-V$ curves. Considering the area of the measured specimens and the density of nanotubes in the AAO template, the average resistance of an individual nanotube can be obtained. The cross-sectional area and length (70 μm) of each individual CNT are easily observed under a microscope, and accordingly, the specific resistivity of a CNT can be calculated. As shown in Table 1, NB-CNTs have the lowest electrical resistivity (5.5 Ω·cm) among these samples. NB-CNTs, N-CNTs (16 Ω·cm), and CB-CNTs (15 Ω·cm) possess, respectively, a resistivity 3, 2, and 2 orders of magnitude lower than the undoped C-CNTs (1.8×10^3 Ω·cm), indicating that B- and N-doping drastically lowers the resistivity of the carbon layer. Since NB-CNTs have a resistivity lower than that of the parent N-CNTs, the resistivity of the B-doped layer would be lower than that of the N-doped layer. These findings give us some clues to probe into the conductivity of the double coaxial CNTs. The crystallinity is likely to be less important than the N- or B-doping for the conductivity of the CNTs. It is commonly accepted that the hopping between microcrystal sheets dominates the conductance behavior in less crystallized materials, such as in the CNTs obtained here.[6] The increase of hopping frequency between the conduction band and valence band, resulting from the doping, is a possible reason for improved conductivity of the doped layers. Moreover, the introduction of N or B into carbon layers in different modes (possibly as an electron acceptor or donor) will exert different influences on the electrical properties. In other words, the conductivity of the carbon layer is tunably consistent with N- or B-doping, and NB-CNTs are of double nature in terms of not only chemical composition but also electrical properties.

In summary, we have successfully prepared the double coaxial CNTs with outer N-doped and inner B-doped multiwalls, which are characterized by the dual electrical properties and chemical activity at their outer and inner layers. Moreover, further study has shown that it is possible to adjust the N or B fraction and respective thicknesses of N-doped and B-doped multiwalls to control these physicochemical properties by changing the CVD conditions. Efforts are underway to confirm if NB-CNTs show $p-n$ junction characteristics through further electrical properties measurement, which is of great interest to constitute nanoelectronic devices.

Acknowledgment. This study was partly supported by the Grant-in-Aid for Exploratory Research 16651055 from the Ministry of Education, Culture, Sport, Science and Technology of Japan.

Supporting Information Available: A schematic illustration of electrical resistance measurement. This material is available free of charge via the Internet at http://pubs.acs.org.

References

(1) Saito, S. *Science* **1997**, *278*, 77.
(2) Terrones, M.; Grobert, N.; Terrones, H. *Carbon* **2002**, *40*, 1665.
(3) Stephan, O.; Ajayan, P. M.; Colliex, C.; Redlich, Ph.; Lambert, J. M.; Bernier, P.; Lefin, P. *Science* **1994**, *266*, 1683.
(4) Xu, W. H.; Kyotani, T.; Pradhan, B. K.; Nakajima, T.; Tomita, A. *Adv. Mater.* **2003**, *15*, 1087.
(5) Yang, Q. H.; Xu, W. H.; Tomita, A.; Kyotani, T. *Chem. Mater.* **2005**, *17*, 2940.
(6) Wei, J.; Hing, P. *Thin Solid Films* **2002**, *410*, 21.

JA052357E